Seasonal sea ice variability in eastern Fram Strait over the last 2,000 years

Patricia Cabedo-Sanz and Simon T Belt*

School of Geography, Earth and Environmental Sciences, Plymouth University, Drake Circus, Plymouth, PL4 8AA, UK

* Author for correspondence

Professor Simon T Belt
Plymouth University
Drake Circus, Plymouth
PL4 8AA
UK

e-mail: sbelt@plymouth.ac.uk
Phone: +44 (0)1752 584959
FAX: +44 (0)1752 584709

Keywords: IP_{25}; sea ice; biomarker; proxy; Late Holocene; Fram Strait

Abstract

We present a high-resolution (ca. 50 yr) biomarker-based reconstruction of seasonal sea ice conditions for the West Svalbard continental margin covering the last ca. 2 kyr. Our reconstruction is based on the distributions of sea ice algal (IP_{25}) and phytoplankton (brassicasterol and HBI III) lipids in marine sediment core MSM5/5-712-1 retrieved in 2007. The individual and combined (PIP_{25}) temporal profiles, together with estimates of spring sea ice concentration (SpSIC (%)) based on a recent calibration, suggest that sea ice conditions during the interval ca. 50-1700 AD may not have been as variable as described in previous reconstructions, with SpSIC generally in the range ca. 35-45%. A slight enhancement in SpSIC (ca. 50%) was identified at ca. 1600 AD, contemporaneous with the Little Ice Age, before declining steadily over the subsequent ca. 400 years to near-modern values (ca. 25%). In contrast to these spring conditions, our data suggest that surface waters during summer months were ice-free for the entire record. The decline in SpSIC in recent centuries is consistent with the known retreat of the winter ice margin from documentary sea ice records. This decrease in sea ice is possibly attributed to enhanced inflow of warm water delivered by the North Atlantic Current and/or increasing air temperatures, as shown in previous marine and terrestrial records. Comparison of our biomarker-based sea ice reconstruction with one obtained previously based on dinocyst distributions in a core from a similar location, reveals partial agreement in the early-mid part of the records (ca. 50–1700 AD), but a notable divergence in the most recent ca. 300 years. We hypothesise that this divergence likely reflects the individual signatures of each proxy method, especially as the biomarker-based SpSIC estimates during this interval (<25%) are much lower

than the threshold level (>50% sea ice cover) used for the dinocyst approach. Alternatively, divergence between outcomes may indicate seasonality shifts in sea ice conditions, such that a combined biomarker-dinocyst approach in future studies might provide further insights into this important parameter.

1. Introduction

1.1 Sea ice and the study region

Sea ice is a critical component of the global climate system, influencing heat, gas and moisture exchange between the oceans and the atmosphere (Thomas and Dieckmann 2010), and further contributing to circulation patterns through brine rejection and freshwater release during ice formation and melt, respectively (e.g. Dickson et al. 2007 and references therein). The observed rapid decline in Arctic sea ice extent and thickness (e.g. Stroeve et al. 2012) has prompted a need to better resolve temporal changes to sea ice in the past, in order that the recent trends can be placed into a better context, and to provide key datasets for improving models of past and future change (e.g. Goosse et al. 2013; Johannessen et al. 2004). From a regional perspective, Fram Strait represents a pivotal study location for investigating past changes to sea ice since it represents the major oceanographic gateway between the Arctic and North Atlantic oceans (Fig. 1a). The two main currents that characterize the region are the North Atlantic Current (NAC) and the East Greenland Current (EGC) (Fig. 1a). Northerly flowing warm Atlantic Water is delivered to the Arctic by the NAC via a principal trajectory along the West Svalbard continental margin, which normally renders eastern Fram Strait relatively free of sea ice, even in

winter. In contrast, western Fram Strait is characterized by cold, ice-laden waters as a result of sea ice export from the Arctic Ocean via the EGC. Arctic Water also flows along the east coast of Svalbard to the south and west of Spitsbergen, delivering sea ice via the East Spitsbergen Current (ESC) (Hopkins 1991; Loeng 1991). The magnitude of heat delivery by the NAC plays a critical role in determining the precise sea ice conditions in eastern Fram Strait. For example, increased Atlantic Water inflow during the last ca. 120 years (Spielhagen et al. 2011) has been associated with a general trend of reduced sea ice cover in the Arctic and, more locally, a northerly retreat of the winter ice margin (Fig. 1b, Divine and Dick 2006). A further impact of the NAC on sea ice conditions in the region, more generally, is that seasonal shifts in the position of the winter and summer ice margins are significantly less pronounced than for the central and eastern Barents Sea, which are dominated by low temperature and salinity Arctic Water (Hopkins 1991). The latter regions also experience seasonal ice cover from autumn to spring, before retreating, rapidly, during late spring/summer. As such, the region as a whole experiences contrasting seasonal sea ice cover (Vinje 1975), which is influenced, in part, by the strength of the NAC (Hopkins 1991).

Motivated, in part, by the sensitivity of oceanographic and atmospheric conditions in Fram Strait towards climatic change, a number of proxy-based studies have been carried out in recent years that have provided new insights into the centennial- and millenial-scale paleoceanographic evolution along the West Svalbard continental margin (e.g. Bonnet et al. 2010; Jernas et al. 2013; Müller and Stein 2014; Müller et al. 2012; Spielhagen et al. 2011; Werner et al. 2013). These investigations have benefited from the recovery of high accumulation rate (and well-dated) marine

sediments, which have enabled the application of an array of biological and mineralogical proxies for the determination of atmospheric and oceanic temperatures, salinity, and sea ice cover (Bonnet et al. 2010; Müller and Stein 2014; Müller et al. 2012; Rueda et al. 2013; Spielhagen et al. 2011; Werner et al. 2011).

Our objective in the current study is to add to the existing suite of previous paleoceanographic investigations for West Svalbard, by presenting a high-resolution (ca. 50 yr) biomarker-based reconstruction of sea ice conditions spanning the last ca. 2 kyr. In particular, we build on recent developments in biomarker-based approaches to sea ice reconstruction by providing both descriptive and semi-quantitative estimates of spring sea ice concentration (SpSIC (%)). Biomarker-based sea ice reconstructions for the West Svalbard margin have been performed previously through analysis of sediments from the same or similar locations, although these focused mainly on longer timeframes (e.g. Holocene and post-LGM; Müller et al. 2012, 2014) and did not provide information for recent centuries. In addition, semi-quantitative estimates of SpSIC were only tentative (Müller et al. 2012). A dinocyst-based record of mean annual sea ice duration (months/yr) for the last 2 kyr for West Svalbard has previously been presented by Bonnet et al. (2010), howwever, and we make comparisons between this and our biomarker-based record as part of the current study.

1.2 Background to biomarker proxy method

In recent years, the organic geochemical marker IP_{25} (Ice Proxy with 25 carbon atoms; Belt et al. 2007) has emerged as a particularly suitable proxy method for

carrying our Arctic sea ice reconstructions, and in the determination of past seasonal sea ice cover, in particular (e.g. Belt and Müller 2013; Belt et al. 2010; Berben et al. 2014; Cabedo-Sanz et al. 2013; Stein et al. 2012). IP_{25} is a mono-unsaturated highly branched isoprenoid (HBI) lipid produced by certain Arctic sea ice diatoms (Brown et al. 2014), and is found commonly in Arctic and sub-Arctic marine sediments underlying seasonal sea ice cover (Müller et al. 2011; Navarro-Rodriguez et al. 2013; Stoynova et al. 2013; Xiao et al. 2013, 2015). Identification of IP_{25} in the geological record (Arctic marine sediments) therefore provides a convincing case for the past occurrence of seasonal sea ice, while variability in IP_{25} content is generally associated with corresponding fluctuations in seasonal sea ice extent (e.g. Belt and Müller 2013). The absence of IP_{25} in Arctic and sub-Arctic settings is less straightforward to interpret, although either of permanent ice cover or ice-free conditions have been suggested as potential settings (e.g. Belt and Müller 2013; Stein et al. 2012; Xiao et al. 2015). In any case, the co-measurement of certain phytoplankton biomarkers (including sterols such as brassicasterol) can provide additional information about low-ice or open-water conditions. In addition, combining IP_{25} and phytoplankton marker concentrations in the form of the so-called PIP_{25} index (Müller et al. 2011) has the potential to provide even more detailed or semi-quantitative estimates of sea ice conditions than from the individual biomarkers alone. The use of brassicasterol as a phytoplankton biomarker when calculating PIP_{25} indices is not without problems, however, since it may also be derived from non-marine sources, and its (generally) much higher sedimentary abundance necessitates the use of a balance factor in the PIP_{25} calculation (see Section 2.2), which can cause problems of consistency, in particular (see Belt and Müller, 2013; Belt et al. 2015 for further details). Since these limitations may not be relevant in all

cases, the adoption of a further phytoplankton marker, possessing a more selective source and which has sedimentary concentrations closer to those of IP_{25}, might represent a suitable complementary approach, at least. Indeed, Belt et al. (2015) recently demonstrated that a further tri-unsaturated HBI lipid ($C_{25:3}$ or HBI III) derived from certain diatoms may be a more suitable phytoplankton marker for use within the PIP_{25} index, following analysis of lipid distributions in surface sediments from the Barents Sea experiencing variable seasonal sea ice cover. Smik et al. (2016) subsequently showed that PIP_{25} indices based on IP_{25} and HBI III (i.e. $P_{III}IP_{25}$) exhibit a strong linear correlation to SpSIC in the Barents Sea, thus providing a potential means of reconstructing semi-quantitative SpSIC (%) estimates for this region, at least. In the current study, we therefore measured concentrations of IP_{25}, brassicasterol and HBI III in a ^{14}C-dated sediment core (MSM5/5-712-1) retrieved from the West Svalbard margin in 2007 and used $P_{III}IP_{25}$ indices together with the recent calibration of Smik et al. (2016) to obtain estimates of SpSIC (%) for the last 2 kyr.

2. Material and methods

2.1 Field methods and chronology

Core MSM5/5-712-1 was recovered from the West Svalbard continental margin (78º54.94 N, 6º46.04 E, water depth 1490.5 m, core length 46 cm; Fig 1a) during cruise leg MSM5/5 on board the R/V *Maria S. Merian* in the summer of 2007. The age model is based on five ^{14}C accelerator mass spectrometry (AMS) radiocarbon dates presented and described previously (Spielhagen et al. 2011).

151

152 *2.2 Biomarker analyses*

153

154 In total, 43 downcore sediment samples were analysed for the biomarkers IP_{25}, HBI
155 III and brassicasterol. Sampling and analysis was carried out at 1 cm intervals
156 representing the last ca. 2 kyr, with a resolution of ca. 50 yr. Biomarker analyses
157 (HBI and sterol lipids) were performed using methods described previously (Belt et
158 al. 2012, 2015). Briefly, two internal standards were added to each freeze-dried
159 sediment sample to permit quantification of lipid biomarkers. 9-octylheptadec-8-ene
160 (9-OHD, 10 µL; 10 µg mL^{-1}) was added for quantification of HBI lipids (IP_{25} and HBI
161 III), while 5α-androstan-3β-ol (10 µL; 10 µg mL^{-1}) was added for quantification of
162 brassicasterol. Samples were then extracted using dichloromethane/methanol (3 x 3
163 mL; 2:1 v/v) and ultrasonication. Following removal of the solvent from the combined
164 extracts using nitrogen, the resulting total organic extracts (TOE) were purified using
165 column chromatography (silica), with HBIs (hexane; 6 mL) and brassicasterol (20:80
166 methylacetate/hexane ; 6 mL) collected as two fractions. Analysis of individual
167 fractions was carried out using gas chromatography-mass spectrometry (GC-MS)
168 and operating conditions were as described previously (e.g. Belt et al. 2012; Brown
169 and Belt 2012). Brassicasterol was derivatized (BSTFA; 50 µL; 70°C; 1h) prior to
170 analysis by GC-MS. Mass spectrometric analyses were carried out either in total ion
171 current (TIC) or single ion monitoring (SIM) mode. The identification of IP_{25} (Belt et
172 al. 2007) and HBI III (Belt et al. 2000) was based on their characteristic GC retention
173 indices and mass spectra. Quantification of lipids was achieved by comparison of
174 mass spectral responses of selected ions (SIM mode, IP_{25}, *m/z* 350; HBI III, *m/z* 346;
175 brassicasterol, *m/z* 470) with those of the internal standards (9-OHD, *m/z* 350; 5α-

androstan-3β-ol, *m/z* 333) and normalized according to their respective response factors and sediment masses (Belt et al. 2012). Analytical reproducibility was monitored using a standard sediment with known abundances of biomarkers for every 20 sediment samples extracted (analytical error 6 %, n = 2). PIP_{25} values were calculated using Equation 1 according to the method of Müller et al. (2011). Similarly, the *c* factor used in the PIP_{25} calculation was obtained from the ratio of the mean concentrations of IP_{25} and each phytoplankton biomarker (i.e. brassicasterol and HBI III; Equation 2). Estimates of SpSIC (%) were calculated using the $P_{III}IP_{25}$ data and the recent calibration of Smik et al. (2016) (Equation 3). Although the study site is located somewhat beyond the main boundary of the region investigated by Smik et al. (2016), we believe that our estimates of SpSIC (and the temporal changes to these) based on this calibration are, nonetheless, realistic, including reasonably good agreement between values from the core-top and known SpSIC obtained from satellite records (see Discussion for further details). A summary of all data can be found in Table 1.

$$PIP_{25} = IP_{25} / (IP_{25} + cP) \quad (1)$$

$$c = \text{mean } IP_{25} / \text{mean P} \quad (2)$$

$$\text{SpSIC (\%)} = (P_{III}IP_{25} - 0.0692) / 0.0107 \quad (3)$$

3. Results

IP_{25}, HBI III and brassicasterol were present in all sedimentary horizons throughout the record although some variability in concentrations was observed for all three biomarkers. Thus, concentrations of IP_{25}, HBI III and brassicasterol were in the

ranges 1.6–3.4, 2.2–4.7 and 340–590 ng g^{-1}, respectively (Fig. 2a-c) and all three biomarkers showed a general in-phase fluctuation from ca. 50 to 1750 AD. An increase in IP_{25}, HBI III and brassicasterol concentrations was observed from ca. 5 to 400 AD, followed by a decline in all three biomarkers from ca. 400 to 700 AD and an interval of relatively low biomarker concentrations between ca. 700 and 800 AD (Fig. 2a-2c). After ca. 800 AD, all biomarkers increased in concentration until ca. 1350 AD, before declining again up to ca. 1750 AD. However, a small lag in the decline of IP_{25} values was observed when compared to those of HBI III and brassicasterol (Fig. 2a-2c). In contrast, IP_{25} concentrations remained generally low after ca. 1750 AD, whereas HBI III and brassicasterol concentrations increased towards the present. In addition, $P_{III}IP_{25}$ values and estimates of SpSIC (%) values remained reasonably consistent (ca. 0.45–0.57 and 35–45 %, respectively) (Fig. 2d, 2e) between ca. 50 and 1400 AD. After ca. 1400 AD, $P_{III}IP_{25}$ and SpSIC values increased to ca. 0.6 and 50 %, respectively, especially between ca. 1500 and 1600 AD, before steadily decreasing towards modern times (Fig. 2d, 2e), where they both reached their lowest values in the entire record.

4. Discussion

4.1 Principal outcomes in terms of sea ice conditions

The occurrence of the sea ice biomarker IP_{25} in all sedimentary horizons analysed provides strong evidence that the MSM5/5-712-1 core site experienced seasonal sea ice cover as a consistent hydrographic feature over the last ca. 2 kyr. P_BIP_{25} and $P_{III}IP_{25}$ profiles were generally in-phase, indicating that both brassicasterol and HBI

III are probably suitable as phytoplankton marker counterparts to IP_{25} for eastern Fram Strait in recent millennia. However, although IP_{25} concentrations and PIP_{25} indices suggest somewhat variable sea ice conditions, the range in our estimates of SpSIC (ca. 25–50%) (Fig. 3d) implies that such variability in sea ice for the West Svalbard margin in recent millennia may have been less extreme than predicted from other proxy records (e.g. Werner et al. 2011), and certainly less than the broad range of sea ice extent for the site throughout the Holocene deduced from a previous study (Müller et al. 2012). For the majority of the early-mid part of the record (ca. 50–1400 AD), estimates of SpSIC are reasonably constant (ca. 35–45 %), before an increase to ca. 50% during the period ca. 1500–1600 AD, contemporaneous with the Little Ice Age (Fig. 3d). Following this increase, SpSIC shows a steady reverse trend after ca. 1660 AD, which extends to the modern era. Interestingly, this declining trend reflects the general reduction in sea ice and a northward retreat of the maximum winter sea ice extent described in documentary records over the last ca. 150 yr (Divine and Dick 2006), while our SpSIC estimates for the top of the core (ca. 25%) are only slightly higher than the mean SpSIC derived from satellite records for this region of Fram Strait over the last ca. 30 yr (10–15 %; NSIDC). Since this interval also corresponds to the upper few centimetres of the core, this slight overestimate in SpSIC might be a consequence of bioturbation in the upper sections, with partial incorporation of older material with higher IP_{25}. Given that $P_{III}IP_{25}$ indices are all well below the lower limit threshold (0.8) suggested recently to be indicative of summer sea ice occurrence (Smik et al., 2016), we also conclude that summer surface waters remained ice-free during the entire record. Further, our data suggest that, since ca. 1900 AD, SpSIC along the West Svalbard margin has diminished to its lowest values in the last 2 kyr, consistent with a coeval and markedly enhanced inflow of warm Atlantic Water to the

Arctic Ocean (Spielhagen et al. 2011) and rising air temperatures derived from marine (Rueda et al. 2013) and terrestrial (e.g. D’Andrea et al. 2012) records.

4.2 Comparisons with other proxy data

The availability of an array of other proxy data for the MSM5/5-712-1 core and related locations enables us to place our new sea ice reconstruction into further context and provide an updated picture of the oceanographic conditions for the West Svalbard margin over the last 2 kyr. Although some consistency between different proxy datasets and alignment with well-known climate epochs (e.g., the Little Ice Age) exists, this is not always the case (e.g. Andersson et al. 2003; Isaksson et al. 2005; Werner et al. 2011). As such, we categorise the temporal paleoceanographic evolution for the last 2 kyr into two main intervals, with reference to certain named epochs, where useful.

4.2.1 Early-mid part of the record (ca. 50–1750 AD)

In the earliest part of the record (ca. 50–700 AD), the increase in IP_{25}, brassicasterol and HBI III concentrations towards ca. 400 AD (Fig. 3a, 3b) suggests a transition from unfavourable conditions for all three biomarkers to one that has a positive influence over the production of both sea ice algae and phytoplankton (viz. ice edge or MIZ conditions). On the basis of enhanced (but variable) planktic foraminiferal fluxes (Fig. 3h), Werner et al. (2011) suggested that this transitional phase represented a general amelioration of conditions from heavy sea ice cover (ca. 120 BC to 1 AD) to one with a fluctuating summer ice margin, and our individual

biomarker data appear consistent with this interpretation. Further, surface and sub-surface temperatures (Rueda et al. 2013; Spielhagen et al. 2011) increase during this phase (Fig. 3f), which are also indicative of a general reduction in sea ice. In contrast, a decline in all three biomarkers from ca. 400 to 700 AD, is accompanied by a slight cooling trend in the alkenone-derived SST record (Fig. 3f), possibly reflecting a return to increased overall sea ice cover. Indeed, between ca. 700 and 800 AD, generally reduced biomarker content coincides with relatively low foraminifera fluxes (Fig. 3h), yet high proportions of polar species (i.e. *N. pachyderma;* Werner et al. 2011). Previously, the latter was interpreted as indicating extended sea ice cover, despite there also being evidence for sub-surface advection of Atlantic Water during the same interval (Werner et al. 2011).

After ca. 800 AD, the increase in all three biomarkers until ca. 1350 AD (Fig. 3a, 3b) suggests a further return to less severe, marginal ice zone (MIZ) conditions, an interpretation supported by a generally warmer surface layer (Fig. 3f) and increases to sub-polar planktic foraminifera (Fig. 3h) (Werner et al. 2011). However, Werner et al. (2011) interpreted the distributions and isotopic composition of planktic foraminifera, together with relatively low IRD from ca. 900 to 1350 AD, as indicative of ice-free conditions, yet our biomarker data suggest seasonal ice cover, even if some estimates of SpSIC from ca. 1100 to 1400 AD are slightly lower (ca. 35 %) than the immediately preceding and subsequent intervals (Fig. 3d). In fact, despite the aforementioned reversible transitions between (apparently) extended sea ice cover and MIZ conditions between ca. 50 and 1300 AD, our estimates of SpSIC remain remarkably consistent (ca. 40%; Fig. 3d) throughout this interval, indicating that factors other than SpSIC are likely to have had influences over biomarker

distributions. Although such factors are currently unidentified, it is interesting, for example, that the alternating trend in biomarker concentrations seen between ca. 50 and 1350 AD is broadly reflected by the alkenone-derived SST record (Fig. 3f), while the seasonal sea ice dynamics may also exert significant control (see later).

The decline in all three biomarkers after ca. 1350 AD indicates a possible further return to enhanced sea ice cover and likely marks the transition into the LIA seen in numerous other North Atlantic marine records (e.g. Andersson et al. 2003; Berstad et al. 2003; Eiríksson et al. 2006; Sicre et al. 2011). However, the decline in IP_{25} exhibits a slight lag compared to the phytoplankton markers (Fig. 3a, 3b) suggesting that the transition in sea ice conditions may have been somewhat different to those described previously. This lag in decreasing IP_{25} concentration is also apparent in the PIP_{25} data, with maximum values around 1600 AD, reflecting a positive deviation in SpSIC to ca. 50%, before declining to more typical values (ca. 40%) after a further ca. 100 yr (Fig. 3d). In addition, this relatively brief interval of enhanced SpSIC is accompanied by lower SST (alkenone) and sSST (planktic foraminifera) (Fig. 3f). After ca. 1600 AD, a decline in the concentration of all three biomarkers possibly suggests a return to enhanced sea ice cover, despite a reduction in the SpSIC and a slight increase in both SST and sSST (Fig. 3f).

A clear feature of the temporal fluctuations in individual biomarker concentrations from ca. 0 to 1750 AD is their in-phase temporal coherence (Fig. 3a, 3b), demonstrating that changes to sea ice conditions impacted somewhat equally (directionally) for both IP_{25} and phytoplankton markers. In some previous IP_{25}-based sea ice reconstructions (e.g. Belt et al. 2015; Cabedo-Sanz et al. 2013; Fahl and

Stein 2012; Müller et al. 2009), often opposing trends in IP_{25} and phytoplankton biomarker profiles have been observed, and interpreted in terms of transitions between intervals of increased sea ice cover (high IP_{25}, low phytoplankton marker) and reduced ice extent (low IP_{25}, high phytoplankton marker). However, consistent with the current data from the West Svalbard margin, Müller et al. (2012) previously reported in-phase changes in IP_{25} and phytoplankton marker concentrations in a Holocene record from the same site and interpreted such a scenario as indicative of a rapidly fluctuating ice margin. Further, Collins et al. (2013) arrived at a similar conclusion for glacial sea ice conditions in the Southern Ocean, adding that in-phase biomarker trends may also be indicative of low sea ice seasonality. For the current study, such an interpretation may, therefore, represent a preferred alternative to one of a more extreme exchange between extended sea ice cover versus marginal ice zone conditions, as described earlier here, and previously (Werner et al. 2011), especially since IP_{25} and the phytoplankton markers are all present throughout the record. In addition, our estimates of SpSIC (ca. 35–45 %) (Fig. 3d) and previous determinations of sea ice duration (ca. 2–6 months/yr) (Fig. 3e) based on dinocysts in a core from the same site (Bonnet et al. 2010), both indicate seasonal, rather than extended, ice cover. In-phase trends within individual biomarker profiles generally have the impact of reducing variability in PIP_{25} (and SpSIC) that may, potentially, lead to an underestimation of the changes in sea ice conditions implied from IP_{25} alone. However, for the MSM5/5-712-1 core, changes in IP_{25} concentration are also relatively small, especially when compared to those seen in longer Holocene records from the same and nearby sites (MSM5/5-712-2 and MSM5/5-723-2; Müller et al. 2012), both of which exhibit similar IP_{25} profiles to our data for the overlapping period (Fig. 3a). Thus, IP_{25} concentration changes by an order of magnitude from the early

to late Holocene in the MSM5/5-712-2 record (Müller et al. 2012), while values covering the last ca. 2 kyr in all three cores only vary by a factor of two, at most (Fig. 3a). Of course, a fluctuating ice margin has much closer parallels with the modern sea ice cycle for the region, with a significantly smaller change in the position of the winter and summer ice margins than, for example, the neighboring Barents Sea (Fig. 1a). Interestingly, peak total foraminifera fluxes (Fig. 3h), previously interpreted as representing ice edge settings by comparison with modern datasets (Werner et al. 2011), also broadly coincide with increased biomarker concentrations, consistent with a strong biological coupling between the surface and sub-surface environments.

4.2.2 The last 250 years (since ca. 1750 AD)

According to our biomarker data, conditions after ca. 1750 AD did not parallel the early-mid part of the record, with generally low IP_{25} concentrations accompanied by increasing phytoplankton marker abundances, especially after ca. 1800 AD. Such changes are particularly apparent through declining PIP_{25} values and SpSIC, but it is also evident that surface (alkenone) and sub-surface (planktic foraminifera) temperatures diverge during this latter part of the LIA, with a clear cooling trend observed for the former (Fig. 3f). The occurrence of generally opposing trends between IP_{25} and HBI III (and brassicasterol) since ca. 1750 AD contrasts the earlier part of the record and previous longer-term Holocene sea ice records from the region (Müller et al. 2012). However, this divergence in IP_{25} and phytoplankton biomarkers is reminiscent of the distributions of IP_{25} and HBI III in surface sediments and downcore records (e.g. core sites 11 and 70; Fig. 1a) from the Barents Sea, with low IP_{25} and high HBI III, in particular, associated with ice-edge retreat within the MIZ

376 during spring (Belt et al., 2015). We suggest, therefore, that from ca. 1750 AD to
377 modern, surface conditions at the West Svalbard margin transcended from higher
378 seasonal sea ice cover (i.e. ca. 40% SpSIC), to a winter ice-edge scenario with
379 reduced SpSIC (ca. 25% or less).
380
381 Our observation of declining SpSIC since ca. 1600 AD is also consistent with the
382 suggestion by Rueda et al. (2013) that reduced surface temperatures and increasing
383 air and sub-surface temperatures, especially in the last ca. 500 yr, may have
384 coincided with a trend of increasing sea ice melt and thus, SpSIC. Increased air
385 temperatures have also been reconstructed for neighboring (terrestrial) West
386 Spitsbergen, with concomitant glacial advance attributed to enhanced precipitation
387 (D’Andrea et al. 2012) that we suggest may also have been associated with reduced
388 sea ice cover. Alternatively, lower SSTs in the recent record may reflect an earlier
389 seasonal bloom due to lower sea ice conditions as suggested previously to explain
390 apparent anomalies in SSTs for the North Icelandic Shelf and coastal settings
391 around Newfoundland in the Labrador Sea (Sicre et al. 2011, 2014). In any case, the
392 apparently increased de-coupling between the surface and sub-surface temperature
393 records since ca. 1750 AD likely reflects a period of most significant change in sea
394 ice conditions, with cooler and fresher surface waters resulting from melting sea ice,
395 possibly as a result of warmer air temperatures as suggested by Rueda et al. (2013).
396 It is also noted that IRD content reached its highest values after ca. 1750 AD (Fig.
397 3g), a further indicator of increasing sea ice melt, although an additional contribution
398 to the IRD budget from icebergs derived from Svalbard glaciers cannot be
399 discounted (e.g. Andersen et al. 1996; Werner et al. 2011).
400

4.2.3 Biomarker versus dinocyst approaches to sea ice reconstruction

As a final discussion point, we compare our biomarker-based sea ice reconstruction with one based on dinocysts in a further core obtained from the same site (Fig. 3e; Bonnet et al. 2010). Inspection of the temporal profile for dinocyst-based sea ice duration (Fig. 3e) with those of biomarkers (individual or PIP_{25}; Fig. 3a-3c) or SpSIC (Fig. 3d) reveals no clear or consistent agreement, even factoring in potential age-control offsets between the two cores. Although some parallels might exist in the early-mid parts of the dinocyst and SpSIC records (ca. 50 to 1400 AD; Fig.3d, 3e), this is not the case for the later profiles, and after ca. 1600 AD, in particular, with reconstructions exhibiting generally opposing trends. In the most recent parts of the records, for example, our estimates of lowest SpSIC align with the northerly retreat of the winter sea ice margin over the last ca. 150 yr (Fig. 1b; Divine and Dick 2006), yet apparently contradict an enhancement in sea ice duration in the dinocyst record (Fig. 3e). Further, the reconstruction of Bonnet et al. (2010) implies ice-free conditions ca. 550–700 AD, while our data suggest SpSIC of ca. 40% for the same interval. Inconsistencies in proxy records are not uncommon, however, and a number of discrepancies have already been reported and discussed for surface temperature and salinity reconstructions based on foraminifera and dinocysts in different cores from the study location (Bonnet et al. 2010; Werner et al. 2011). Such differences are not necessarily straightforward to resolve, but may potentially arise from influences associated with seasonally-dependent proxy responses, changes to water column sub-structure, variable depth habitat of native flora and fauna, or appropriateness of transfer functions, which may exhibit a strong regional dependence. Inconsistencies between biomarker- and dinocyst-based sea ice

426 reconstructions have been reported previously and loosely attributed to the possible
427 different signatures that each proxy represents (e.g. Belt and Müller 2013; de Vernal
428 et al. 2013a; Ledu et al. 2010; Polyak et al. in press). Outcomes from the current
429 study might help further direct this debate. For example, the dinocyst-based method
430 yields semi-quantitative estimates of sea ice *duration* in months of sea ice (with >50
431 % cover)/yr (de Vernal et al. 2013b), while the corresponding reconstructions based
432 on IP_{25} are intrinsically associated with spring sea ice conditions (Belt et al. 2013;
433 Brown et al. 2011) and, more quantitatively, seasonal (spring) sea ice *concentration*,
434 as described here and previously (Belt et al. 2015; Müller et al. 2011; Navarro-
435 Rodriguez et al. 2013; Smik et al. 2016; Xiao et al. 2015). For the current study, we
436 also note that SpSIC is almost exclusively below the threshold level for dinocyst-
437 based methods (>50% sea ice cover) in any case, so differences between outcomes
438 are not entirely unexpected. It is also feasible that while there might be some
439 scenarios for which sea ice duration and SpSIC are reasonably in-phase, divergence
440 in their respective proxy records may reflect an effective de-coupling between them,
441 especially during intervals of amplified seasonality. For example, for the West
442 Svalbard margin, we speculate that increasing sea ice duration, yet declining SpSIC,
443 seen in the last ca. 300 years, may have arisen due to larger seasonal shifts
444 between generally colder winters and warmer summer temperatures that would have
445 particularly impacted on spring ice melt. Consistent with this suggestion, increasing
446 air temperatures from marine (Rueda et al. 2013) and terrestrial (D’Andrea et al.
447 2012) records for the region since ca. 1600 AD coincide with the reduction in SpSIC
448 shown here. The combination of new biomarker-based approaches for estimating
449 SpSIC with complementary methods of determining sea ice duration may, therefore,
450 offer additional insights into seasonal shifts in sea ice occurrence that are not

451 necessarily available from either individual proxy. Such approaches would clearly
452 benefit from further dinocyst and biomarker investigations on the same sediments.
453
454 **5. Conclusions**
455
456 Our biomarker-based reconstruction of sea ice conditions for the West Svalbard
457 continental margin covering the last ca. 2 kyr, suggests that changes to sea ice
458 conditions during this interval may not have been as extreme as reported in previous
459 proxy-based studies, especially for the interval ca. 50–1700 AD, with SpSIC
460 generally ca. 40% throughout. An increase in SpSIC to ca. 50% was observed at ca.
461 1600 AD, however, which we attribute to slightly enhanced sea ice cover during the
462 LIA. SpSIC returned to more typical values at ca. 1750 AD, before declining further
463 towards modern values (ca. 25%), consistent with observational records of a
464 northerly retreat of the winter sea ice limit in the last ca. 150 yr (Divine and Dick
465 2006). The general in-phase behavior of the sea ice algal and phytoplankton
466 markers observed for the majority of the record (ca. 50–1750 AD), is indicative of a
467 fluctuating ice margin and relatively low sea ice seasonality. In contrast, a
468 divergence in trends of the same biomarkers since ca. 1750 AD is interpreted in
469 terms of an amplified seasonal sea ice cycle and a rapid ice edge retreat within the
470 MIZ during the spring; thus providing a model for the sea ice conditions for the West
471 Svalbard margin in recent centuries. Such a contrast in the relative temporal trends
472 of sea ice and pelagic biomarkers has been observed in related sea ice
473 reconstructions (e.g. Belt et al. 2015; Müller et al. 2009) and may prove to be an
474 additionally useful tool when deducing or refining paleo sea ice conditions.
475 Improvements to such paleo sea ice descriptions, and temporal changes to these,

476 will also help in the further refinement of other proxy-based inferences of surface
477 environments, in particular, and may potentially help clarify (or resolve)
478 reconstructions of broader water column features for sea ice covered settings.
479
480 **6. Acknowledgements**
481
482 We thank the University of Plymouth for financial support and Dr Robert Spielhagen
483 for sampling the MSM5/5-712-1 core. We are also grateful to two anonymous
484 reviewers who provided a number of useful comments that helped improve the
485 quality of the manuscript. This work is a contribution to the CASE Initial Training
486 Network funded by the European Community's 7th Framework Programme FP7
487 2007/2013, Marie-Curie Actions, under Grant Agreement No. 238111.

7. References

Andersen ES, Dokken TM, Elverhøi A, Solheim A, Fossen I (1996) Late Quaternary sedimentation and glacial history of the western Svalbard continental margin Marine Geology 133:123-156

Andersson C, Risebrobakken B, Jansen E, Dahl SO (2003) Late Holocene surface ocean conditions of the Norwegian Sea (Vøring Plateau) Paleoceanography 18:1044

Belt ST, Allard WG, Massé G, Robert J-M, Rowland SJ (2000) Highly branched isoprenoids (HBIs): identification of the most common and abundant sedimentary isomers Geochimica et Cosmochimica Acta 64:3839-3851

Belt ST, Brown TA, Navarro Rodriguez A, Cabedo Sanz P, Tonkin A, Ingle R (2012) A reproducible method for the extraction, identification and quantification of the Arctic sea ice proxy IP_{25} from marine sediments Analytical Methods 4:705-713

Belt ST, Brown TA, Ringrose AE, Cabedo-Sanz P, Mundy CJ, Gosselin M, Poulin M (2013) Quantitative measurement of the sea ice diatom biomarker IP_{25} and sterols in Arctic sea ice and underlying sediments: Further considerations for palaeo sea ice reconstrucion Organic Geochemistry 62:33-45

Belt ST, Cabedo-Sanz P, Smik L, Navarro-Rodriguez A, Berben SM, Knies J, Husum K (2015) Identification of paleo Arctic winter sea ice limits and the marginal ice zone: Optimised biomarker-based reconstructions of late Quaternary Arctic sea ice Earth and Planetary Science Letters 431:127-139

Belt ST, Massé G, Rowland SJ, Poulin M, Michel C, LeBlanc B (2007) A novel chemical fossil of palaeo sea ice: IP_{25} Organic Geochemistry 38:16-27

Belt ST, Müller J (2013) The Arctic sea ice biomarker IP_{25}: a review of current understanding, recommendations for future research and applications in palaeo sea ice reconstructions Quaternary Science Reviews 79:9-25

Belt ST et al. (2010) Striking similarities in temporal changes to spring sea ice occurrence across the central Canadian Arctic Archipelago over the last 7000 years Quaternary Science Reviews 29:3489-3504

Berben SMP, Husum K, Cabedo-Sanz P, Belt ST (2014) Holocene sub centennial evolution of Atlantic water inflow and sea ice distribution in the western Barents Sea Climate of the Past 10:181-198

Berstad IM, Sejrup HP, Klitgaard‐Kristensen D, Haflidason H (2003) Variability in temperature and geometry of the Norwegian Current over the past 600 yr; stable isotope and grain size evidence from the Norwegian margin Journal of Quaternary Science 18:591-602

523 Bonnet S, de Vernal A, Hillaire-Marcel C, Radi T, Husum K (2010) Variability of sea-
524 surface temperature and sea-ice cover in the Fram Strait over the last two millennia
525 Marine Micropaleontology 74:59-74

526 Brown TA, Belt ST (2012) Identification of the sea ice diatom biomarker IP_{25} in Arctic
527 benthic macrofauna: direct evidence for a sea ice diatom diet in Arctic heterotrophs
528 Polar Biology 35:131-137

529 Brown TA, Belt ST, Philippe B, Mundy CJ, Massé G, Poulin M, Gosselin M (2011)
530 Temporal and vertical variations of lipid biomarkers during a bottom ice diatom
531 bloom in the Canadian Beaufort Sea: further evidence for the use of the IP_{25}
532 biomarker as a proxy for spring Arctic sea ice Polar Biology 34:1857-1868

533 Brown TA, Belt ST, Tatarek A, Mundy CJ (2014) Source identification of the Arctic
534 sea ice proxy IP_{25} Nature communications 5

535 Cabedo-Sanz P, Belt ST, Knies J, Husum K (2013) Identification of contrasting
536 seasonal sea ice conditions during the Younger Dryas Quaternary Science Reviews
537 79:74-86

538 Collins LG, Allen CS, Pike J, Hodgson DA, Weckström K, Massé G (2013)
539 Evaluating highly branched isoprenoid (HBI) biomarkers as a novel Antarctic sea-ice
540 proxy in deep ocean glacial age sediments Quaternary Science Reviews 79:87-98

541 D’Andrea WJ, Vaillencourt DA, Balascio NL, Werner A, Roof SR, Retelle M, Bradley
542 RS (2012) Mild Little Ice Age and unprecedented recent warmth in an 1800 year lake
543 sediment record from Svalbard Geology 40:1007-1010

544 de Vernal A, Gersonde R, Goosse H, Seidenkrantz M-S, Wolff EW (2013a) Sea ice
545 in the paleoclimate system: the challenge of reconstructing sea ice from proxies – an
546 introduction Quaternary Science Reviews 79:1-8

547 de Vernal A, Rochon A, Fréchette B, Henry M, Radi T, Solignac S (2013b)
548 Reconstructing past sea ice cover of the Northern Hemisphere from dinocyst
549 assemblages: status of the approach Quaternary Science Reviews 79:122-134

550 Dickson R, Rudels B, Dye S, Karcher M, Meincke J, Yashayaev I (2007) Current
551 estimates of freshwater flux through Arctic and subarctic seas Progress in
552 Oceanography 73:210-230

553 Divine DV, Dick C (2006) Historical variability of sea ice edge position in the Nordic
554 Seas J Geophys Res 111:C01001

555 Eiríksson J et al. (2006) Variability of the North Atlantic Current during the last 2000
556 years based on shelf bottom water and sea surface temperatures along an open
557 ocean/shallow marine transect in western Europe The Holocene 16:1017-1029

558 Fahl K, Stein R (2012) Modern seasonal variability and deglacial/Holocene change
559 of central Arctic Ocean sea-ice cover: New insights from biomarker proxy records
560 Earth and Planetary Science Letters 351–352:123-133

561 Goosse H, Roche DM, Mairesse A, Berger M (2013) Modelling past sea ice changes
562 Quaternary Science Reviews 79:191-206

563 Hopkins TS (1991) The GIN Sea - a synthesis of its physical oceanography and
564 literature review 1972 - 1985 Earth Science Reviews 30:175-318

565 Isaksson E et al. (2005) Two ice-core $\delta^{18}O$ records from Svalbard illustrating climate
566 and sea-ice variability over the last 400 years The Holocene 15:501-509

567 Jernas P, Klitgaard Kristensen D, Husum K, Wilson L, Koç N (2013)
568 Palaeoenvironmental changes of the last two millennia on the western and northern
569 Svalbard shelf Boreas 42:236-255

570 Johannessen OM et al. (2004) Arctic climate change: observed and modelled
571 temperature and sea ice variability Tellus A 56:328-341

572 Ledu D, Rochon A, de Vernal A, St-Onge G (2010) Holocene paleoceanography of
573 the northwest passage, Canadian Arctic Archipelago Quaternary Science Reviews
574 29:3468-3488

575 Loeng H (1991) Features of the physical oceanographic conditions of the Barents
576 Sea Polar research 10:5-18

577 Müller J, Massé G, Stein R, Belt ST (2009) Variability of sea-ice conditions in the
578 Fram Strait over the past 30,000 years Nature Geoscience 2:772-776

579 Müller J, Stein R (2014) High-resolution record of late glacial and deglacial sea ice
580 changes in Fram Strait corroborates ice–ocean interactions during abrupt climate
581 shifts Earth and Planetary Science Letters 403:446-455

582 Müller J, Wagner A, Fahl K, Stein R, Prange M, Lohmann G (2011) Towards
583 quantitative sea ice reconstructions in the northern North Atlantic: A combined
584 biomarker and numerical modelling approach Earth and Planetary Science Letters
585 306:137-148

586 Müller J, Werner K, Stein R, Fahl K, Moros M, Jansen E (2012) Holocene cooling
587 culminates in sea ice oscillations in Fram Strait Quaternary Science Reviews 47:1-14

588 Navarro-Rodriguez A, Belt ST, Knies J, Brown TA (2013) Mapping recent sea ice
589 conditions in the Barents Sea using the proxy biomarker IP_{25}: implications for palaeo
590 sea ice reconstructions Quaternary Science Reviews 79:26-39

591 Polyak L, Belt ST, Cabedo-Sanz P, Yamamoto M, Park Y-H (in press) Holocene sea-
592 ice conditions and circulation at the Chuckchi-Alaskan margin, Arctic Ocean, inferred
593 from biomarker proxies The Holocene

594 Rueda G, Fietz S, Rosell-Melé A (2013) Coupling of air and sea surface
595 temperatures in the eastern Fram Strait during the last 2000 years The Holocene
596 23(5):692-698

597 Sicre MA et al. (2011) Sea surface temperature variability in the subpolar Atlantic
598 over the last two millennia Paleoceanography 26:PA4218

599 Sicre MA et al. (2014) Labrador current variability over the last 2000 years Earth and
600 Planetary Science Letters 400:26-32

601 Smik L, Cabedo-Sanz P, Belt ST (2016) Semi-quantitative estimates of paleo Arctic
602 sea ice concentration based on source-specific highly branched isoprenoid alkenes:
603 A further development of the PIP_{25} index Organic Geochemistry 92:63-69

604 Spielhagen RF et al. (2011) Enhanced modern heat transfer to the Arctic by warm
605 Atlantic water Science 331:450-453

606 Stein R, Fahl K, Müller J (2012) Proxy Reconstruction of Cenozoic Arctic Ocean
607 Sea-Ice History–from IRD to IP_{25}– Polarforschung 82:37-71

608 Stoynova V, Shanahan TM, Hughen KA, de Vernal A (2013) Insights into Circum-
609 Arctic sea ice variability from molecular geochemistry Quaternary Science Reviews
610 79:63-73

611 Stroeve JC, Serreze MC, Holland MM, Kay JE, Malanik J, Barrett AP (2012) The
612 Arctic’s rapidly shrinking sea ice cover: a research synthesis Climatic Change
613 110:1005-1027

614 Thomas DN, Dieckmann GS (2010) Sea Ice. second edn. WIley Blackwell
615 Publishing, New York

616 Vinje T (1975) Sea ice conditions in the European sector of the marginal seas of the
617 Arctic, 1966–1975 Norsk Polarinst, Arbok:163-174

618 Werner K, Spielhagen RF, Bauch D, Hass HC, Kandiano E (2013) Atlantic Water
619 advection versus sea‐ice advances in the eastern Fram Strait during the last 9 ka:
620 Multiproxy evidence for a two‐phase Holocene Paleoceanography 28:283-295

621 Werner K, Spielhagen RF, Bauch D, Hass HC, Kandiano E, Zamelczyk K (2011)
622 Atlantic Water advection to the eastern Fram Strait—Multiproxy evidence for late
623 Holocene variability Palaeogeography, Palaeoclimatology, Palaeoecology 308:264-
624 276

625 Xiao X, Fahl K, Müller J, Stein R (2015) Sea-ice distribution in the modern Arctic
626 Ocean: Biomarker records from trans-Arctic Ocean surface sediments Geochimica et
627 Cosmochimica Acta 155:16-29

628 Xiao X, Fahl K, Stein R (2013) Biomarker distributions in surface sediments from the
629 Kara and Laptev seas (Arctic Ocean): indicators for organic-carbon sources and sea-
630 ice coverage Quaternary Science Reviews 79:40-52

8. Figure Legends

Figure 1: (a) Map showing the core location under study (yellow diamond): MSM5/5-712-1 (712-1). Other cores mentioned in this paper (black dots) are: MSM5/5-723-2 (723-2, Müller et al. 2012), MSM5/5-712-2 (712-2, Müller et al. 2012), JM09-KA11-GC (11, Belt et al. 2015) and NP05-11-70GC (70, Belt et al. 2015). The core site described in Bonnet et al. (2010) is at the same location as core 712-1. The main ocean currents are the cold East Greenland Current (EGC), carried southwards along the east coast of Greenland, and the relatively warm North Atlantic Current (NAC) that flows northward along the northern Norwegian shelf and continues into the Arctic Ocean via the West Spitsbergen Current (WSC). The cold East Spitsbergen Current (ESC) is also indicated. The median sea ice extent (>15% monthly mean concentration) for March (black line) and September (magenta line) are shown for the period 1981–2010 (National Snow and Ice Data Center, Boulder, Colorado); (b) Map showing average April location of the sea ice margins at 1870–1920 AD (black line), 1921–1961 AD (blue line), 1962–1988 AD (magenta line) and 1989–2002 AD (red line), (http://nsidc.org/data/gis/data.html; data based on Divine and Dick, 2006). The five ^{14}C accelerator mass spectrometry (AMS) radiocarbon dates used for the age model (Spielhagen et al. 2011) are shown as black diamonds.

Figure 2: Temporal concentration profiles of (a) IP_{25}; (b) HBI III; (c) Brassicasterol; (d) PIP_{25} indices calculated using phytoplankton markers HBI III ($P_{III}IP_{25}$) and brassicasterol ($P_{B}IP_{25}$); (e) SpSIC (%) based on Smik et al. (2016).

Figure 3. Compilation of proxy data from MSM5/5-712-1 and related cores from the study region. Data are for MSM5/5-712-1 unless otherwise stated. (a) IP_{25} concentrations in MSM5/5-712-1 (black line), MSM5/5-712-2 (red line, Müller et al. 2012) and MSM5/5-723-2 (blue line, Müller et al. 2012); (b) HBI III and brassicasterol concentrations; (c) PIP_{25} indices calculated using phytoplankton markers HBI III ($P_{III}IP_{25}$) and brassicasterol ($P_{B}IP_{25}$); (d) SpSIC (%) based on Smik et al. (2016); (e) Dinocyst-based sea ice cover (months/yr) derived from a further core at the same location as MSM5/5-712-1 (Bonnet et al. 2010); (f) SST and sSST (ºC) derived from alkenones (Rueda et al. 2013) and planktic foraminifera (Spielhagen et al. 2011), respectively; (g) IRD in the 150–250 µm fraction (Werner et al. 2011); (h) fluxes of polar and subpolar planktic foraminifers (100–250 µm fraction) (Spielhagen et al. 2011; Werner et al. 2011). The five ^{14}C accelerator mass spectrometry (AMS) radiocarbon dates used for the age model (Spielhagen et al. 2011) are shown as black diamonds.

Figure 1:

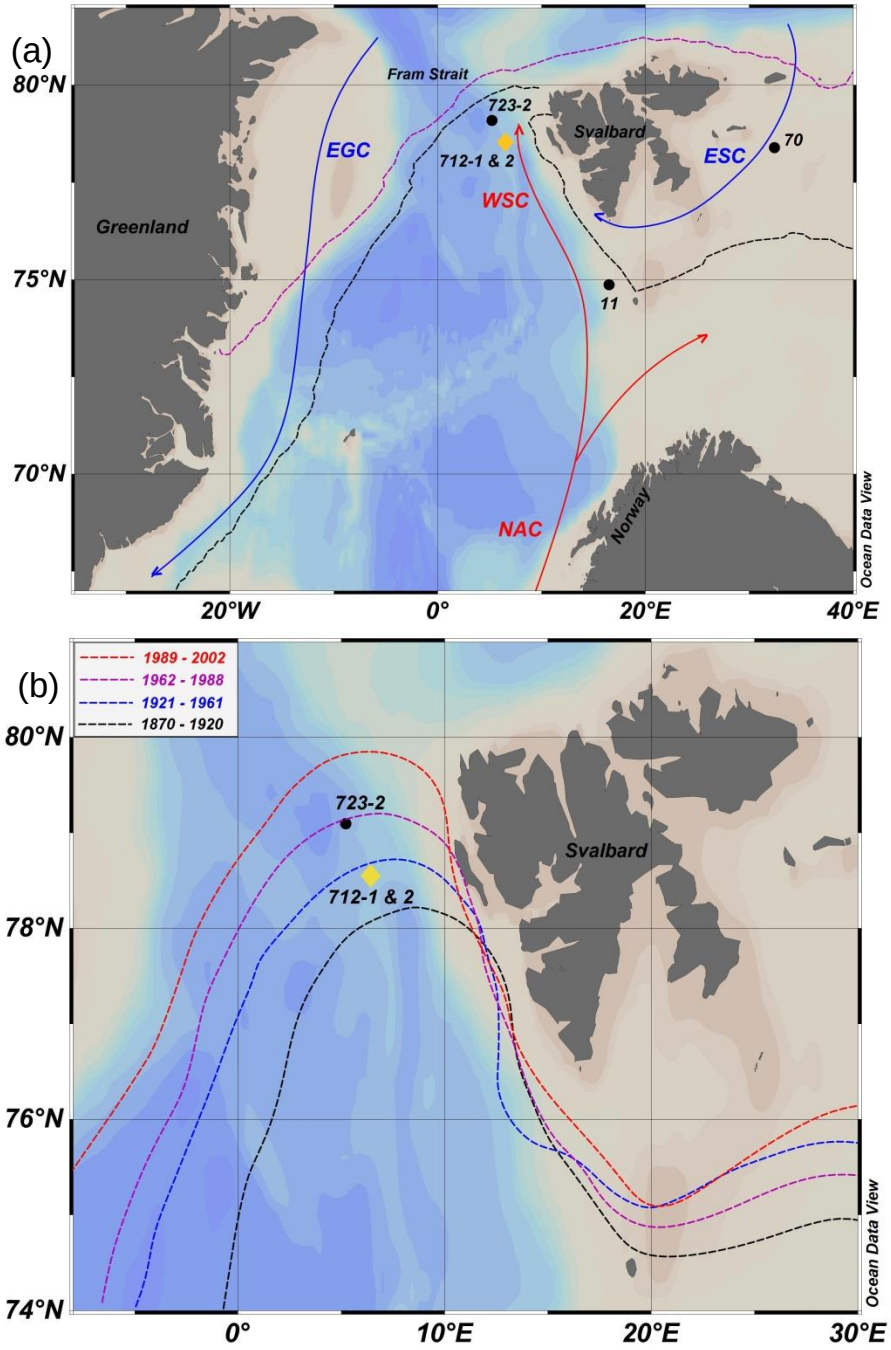

Figure 2:

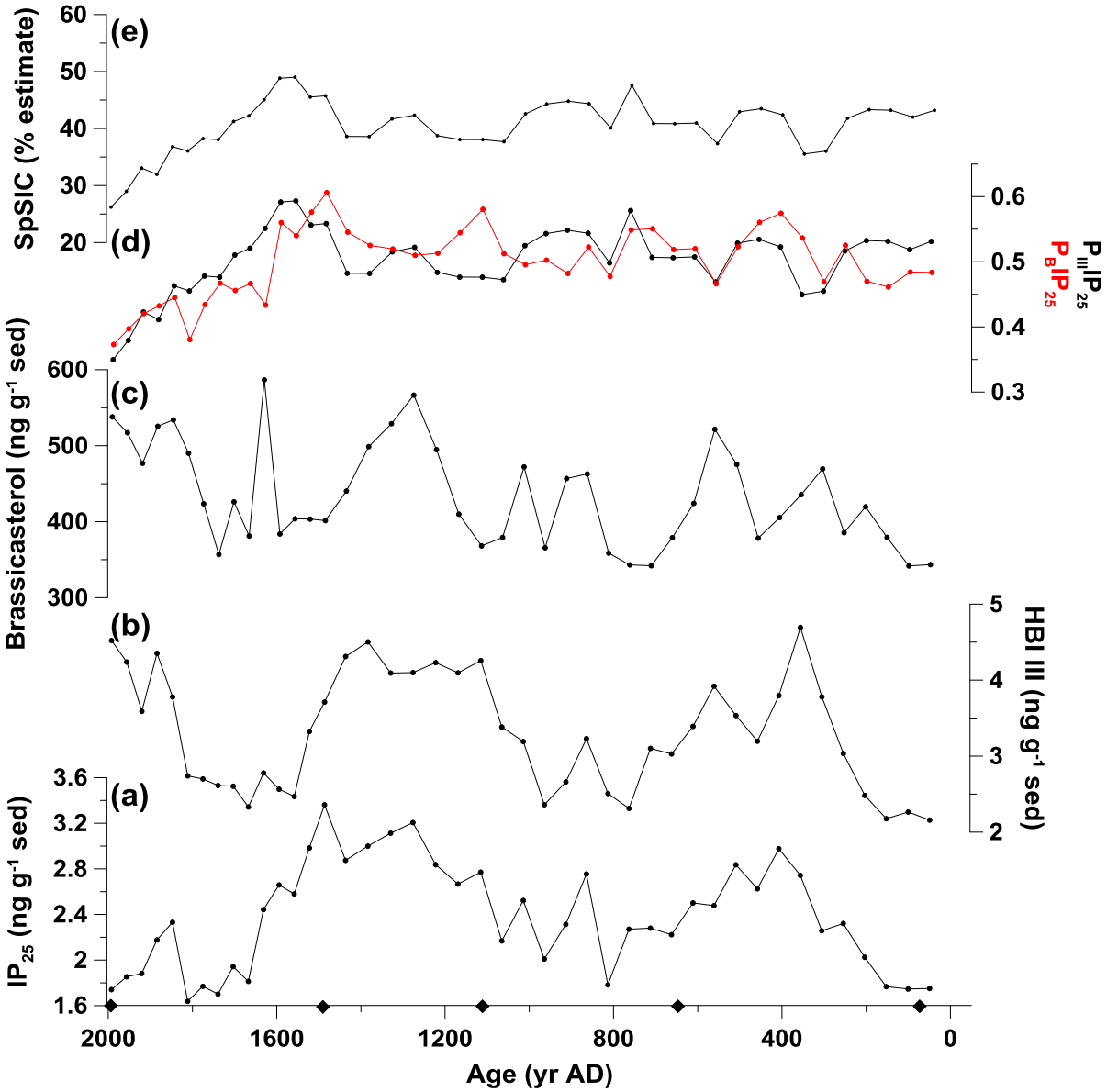

Figure 3: